

A novel synthesis of 4-toluene 9H-carbazole-9-carbodithioate, electropolymerization and impedance study

M. Ates^{1*}, N. Uludag¹, T. Karazehir^{1,2}, F. Arican¹

¹Department of Chemistry, Faculty of Arts and Sciences, Namik Kemal University, Degirmenalti Campus, 59030 Tekirdag, Turkey

²Department of Chemistry, Faculty of Arts and Sciences, Istanbul Technical University, Maslak, Istanbul, Turkey

Received 5 January 2014; accepted in revised form 8 March 2014

Abstract. A novel synthesis of 4-toluene 9H-carbazole-9-carbodithioate (TCzC) was chemically synthesized and characterized by Fourier Transform Infrared (FTIR), proton nuclear magnetic resonance (¹H-NMR), and carbon nuclear magnetic resonance (¹³C-NMR) spectroscopies. Specific (C_{sp}) and double layer capacitances (C_{dl}) of the electro-coated poly(carbazole) and poly(TCzC) films were obtained on glassy carbon electrode (GCE) by impedimetric method with DC potential from -0.1 to $+1.0$ V by increasing potential of 0.2 V. The polymers were characterized by Cyclic voltammetry (CV), Fourier transform infrared reflectance-attenuated total reflection spectroscopy (FTIR-ATR), Atomic force microscopy (AFM), and Electrochemical impedance spectroscopy (EIS). The use of additional variable (DC potential) helped to disambiguate the equivalent circuit model of $R(C(R(Q(RW))))(CR)$. Simulation results were compared with experimental data. In this study, substituted group effects of CS₂ and tosyl on carbazole polymer were investigated by EIS technique. CS₂ group together with tosyl group in the structure of carbazole decreased the specific capacitance value ($C_{sp} = 0.43$ mF·cm⁻²) compared to PCz ($C_{sp} = 1.44$ mF·cm⁻²). Electropolymerization formation was seriously affected by substituted groups of CS₂ and tosyl on conjugation system because of the electron donor and acceptor ability.

Keywords: coatings, functional polymer, electrochemical impedance spectroscopy, electropolymerization, conducting polymer

1. Introduction

Among conducting polymers, polycarbazoles are known for their good electro-activity [1, 2] and thermal [3–5], electrical [6], photo-physical [7], and electrochromic properties [8]. They have been suggested for a number of applications, such as electroluminescent devices [9], sensors [10, 11], redox catalysts [12], and electrochromic displays [13]. The functional groups, such as amino, imino and sulfonic groups have been performed for achieving new polymers which meet the criteria of commercial applications [14–16]. There are many novel

syntheses of functional polycarbazole papers. 3,6-bis (2,3-dihydrothieno [3,4-b][1,4] dioxin-5-yl)-9-tosyl-9H-carbazole [17], 5-(3,6-Dibromo-9H-carbazole-9-yl)-pentane nitrile [18], 9-tosyl-9H-carbazole [19], 9-tosyl-9H-carbazole-co-pyrrole [20], N-(1,4-Dimethyl-9H-carbazole-3-ylmethyl)-N-tosyl aminoacetaldehyde diethyl acetal [21], ethyl 4-hydroxy-9-tosyl-9H-carbazole-3-carboxylate [22], 4-[2-carbazole-3-yl] vinyl] pyridium tosylate [23], N-(o-ethynyl)phenylnamides and arylnamides [24] and 9-(4-nitrophenylsulfonyl)-9H-carbazole [25] were given in literature. The synthesis was per-

*Corresponding author, e-mail: mates@nku.edu.tr
© BME-PT

formed especially with donor-acceptor group, which supported electron rich and poor region on the polymer skeleton [26].

Electrochemical impedance spectroscopy (EIS) is one of the most frequently used analytical tools for the characterization of capacitors or supercapacitors [27]. EIS is used to explain behavior of modified electrodes explaining two models, which are known as uniform [28] and porous medium [29]. In this study, porous medium was evaluated by EIS. At present, the electrode materials for supercapacitors have been widely investigated especially for carbon materials such as activated carbons, the mostly widely used electrode materials due to their large surface area, relatively good electrical properties and moderate cost [30–32]. Among the carbon materials, carbon nanotubes (CNT) are considered to be potential candidates as the electrodes in supercapacitor, due to their high accessible surface, chemical stability, excellent mechanical properties, good electrical conductivity, and unique pore structure [33, 34]. The other electrode materials such as transition metal oxides and conducting polymer [35, 36] are being widely investigated to improve the specific capacitance and the energy density of supercapacitor [37, 38].

Herein, in this study, we principally synthesized CS₂ and tosyl group of substituent of carbazole monomer and compare the effects of these functional groups on EIS properties. Also we investigated the equivalent circuit model of $R(C(R(Q(RW))))(CR)$ with Kramers-Kronig transform to fit the experimental and theoretical data. As a result, this paper presents a new approach of circuit Modeling and capacitive behavior of a novel polymer synthesis by using EIS technique.

2. Experimental

2.1. Materials

Carbazole (Alfa Aesar, USA), sodium hydroxide (NaOH), carbon disulfide (Aldrich, USA), p-toluenesulfonyl chloride (Aldrich, USA) were received without further purification. Dichloromethane (CH₂Cl₂), dimethylsulfoxide (DMSO), diethyl ether, acetonitrile (CH₃CN), tetraethylammonium tetrafluoroborate (TEABF₄) were supplied from Merck Chemical Co. (Germany) and they were used as received. Silica gel, used for synthesis experiments, was described as an efficient and reusable catalyst.

2.2. Electrochemical tests

Cyclic voltammetry (CV) was performed by using PARSTAT 2273, USA (software: powersuit and Faraday cage: BASI Cell Stand C3, West Lafayette, Indiana, USA) in a three electrode configuration, which employed glassy carbon electrode (GCE) (area: 0.07 cm²) as the working electrode, platinum wire as the counter electrode and Ag/AgCl (3.5 M) as the reference electrode. All electrochemical experiments were carried out at 20±1°C.

2.3. Structure characterization

Modified carbon fiber microelectrode (CFME) was characterized by Fourier transform infrared- attenuated total reflection (FTIR-ATR) spectroscopy (Perkin Elmer, Spectrum One B, with an universal ATR sampling accessory (4000–550 cm⁻¹) with a diamond and ZnSe crystal, USA). The Atomic force microscopy (AFM) images were obtained with Park System XE100 Suwon, Korea. In all AFM analysis, the non-contact mode was employed by using Al coated high resonance frequency silicon tips (265–400 kHz) with 4 μm thickness, 35 μm mean width, 125 μm length and 20–75 N/m force constant. High resolution images (1024×1024 pixels) and the raw data were collected by the XEI image. Melting point was determined in a capillary tube on Electro thermal IA 9000 apparatus and uncorrected (Stone Staffordshire, UK). Mass spectra were determined by means of Agilent 5973 model of GC-MS (Santa Clara, CA, USA).

2.4. Electrochemical impedance spectroscopy and modeling

Electrochemical impedance spectroscopic (EIS) measurements were performed for Cz and TCzC in the initial molar concentration of 3.0 mM in 0.1 M tetraethylammonium tetrafluoroborate (TEABF₄)/dichloromethane (CH₂Cl₂) – acetonitrile (CH₃CN) volume ratio of (8:2). EIS measurements were done in monomer-free electrolyte solution with perturbation amplitude of 10 mV and DC potential from –0.1 to +1.0 V on glassy carbon electrode (GCE) over a frequency range of 0.01 Hz to 100 kHz with PARSTAT 2273 model Potansiostat/galvanostat. All measurements began at the open circuit potential, modified polymer films were allowed to equilibrate for ~10 min at each potential before being measured. The equivalent circuit model of $R(C(R(Q(RW))))(CR)$

was taken by Kramers-Kronig Transform (ZSimpwin programme).

3. Results and discussion

3.1. Synthesis procedure

A suspension of NaOH (1.2 g, 30 mmoles) in dimethylsulfoxide (DMSO, 150 mmoles) was prepared. Afterwards, carbazole (5 g, 29.9 mmoles) was added under vigorous stirring. The reaction mixture was stirred for 2 hours at room temperature. Carbondisulfide (2.2 g, 30 mmoles) was added dropwise into the mixture, and the resultant reddish solution was stirred for 4 hours at room temperature, and then by adding slowly p-toluensulfonylchloride (5.7 g, 30 mmoles) in DMSO (30 mL). The final mixture was stirred for a night. The resultant reaction mixture which was poured into large amount of water and yellow solid was obtained by filtration. The crude product was purified by silica gel chromatography and crystallised from diethyl ether. The resultant mass was 6.5 g. 4-toluene 9*H*-carbazole-9-carbodithioate (yield: 59%) was obtained at the melting temperature of 194°C and molecular weight of 337.53 g/mol obtained by coupled gas chromatography and mass spectrometry (GC-MS) (Figure 1).

As a basis for the synthetic approaches to 4-toluene-9*H*-carbazole-9-carbodithioate was synthesized from carbazole by using similar methods given in the literatures [39, 40]. The spectra of dithiocarbamates obtained were identical to those of the produced in the above literatures.

C=S bond on CS₂ group connected with carbazole and electron pair on nitrogen atom showed a reso-

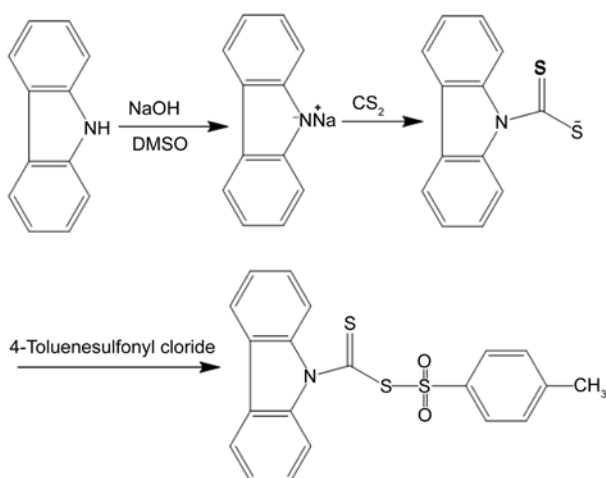


Figure 1. Synthesis procedure of 4-toluene 9*H*-carbazole-9-carbodithioate

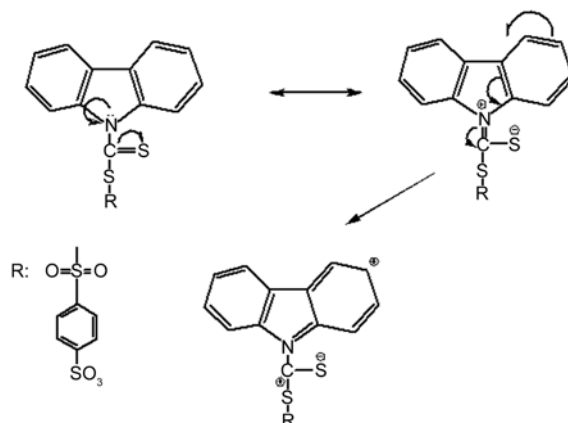


Figure 2. Resonance formation of 4-toluene 9*H*-carbazole-9-carbodithioate

nance structure and formed an active side with positive (+) charges on the carbazole structure of 3 and 6 position. An easy polymer formation was supplied by cationic polymerization with conjugation system. Polymerization formation was crucially affected by substituted groups on conjugation system due to electron donor and acceptor groups as shown in Figure 2.

Carbazole was treated with NaOH and carbondisulfide in the presence of DMSO then added 4-methyl benzene-1-sulfonylchloride to obtain 4-toluene-9*H*-carbazole-9-carbodithioate (59% yield). 4-toluene-9*H*-carbazole-9-carbodithioate was determined by FTIR, ¹NMR, and ¹³C-NMR.

3.2. Characterisation of 4-toluene

9*H*-carbazole-9-carbodithioate monomer

FT-IR analysis (potassium bromide): ν₃₀₅₈ cm⁻¹ (aromatic C-H), 1593 cm⁻¹ (aromatic C=C), 1487 cm⁻¹ (aromatic C=C), 1435 cm⁻¹ (aromatic C=C). The peak of N-H at 3000–3500 cm⁻¹ was not observed in the FTIR spectrum. It proved the insertion of the CS₂ group into the carbazole structure as shown in Figure 3.

¹H-NMR (deuteriochloroform) spectrum of TCzC: δ 2.31 (s, CH₃), 7.07–7.12 (d, 2H, aromatic C-H), 7.25–7.33 (d, 2H, aromatic C-H), 7.35–7.41 (m, 2H, aromatic C-H), 7.46–7.90 (m, 2H, aromatic C-H), 8.31–8.34 (d, 2H, aromatic C;H). 4-toluene-9*H*-carbazole-9-carbodithioate was determined by NMR experiments and FT-IR spectroscopy. The most characteristic value of its ¹H-NMR spectrum was a singlet of methyl proton peaks at 2.31 ppm, as well as between 7.07–7.90 ppm aromatic protons.

¹H-NMR (deuteriochloroform) spectrum of Cz: δ 7.21–7.25 (m, 4H, aromatic CH), 7.39–7.51 (m, 4H,

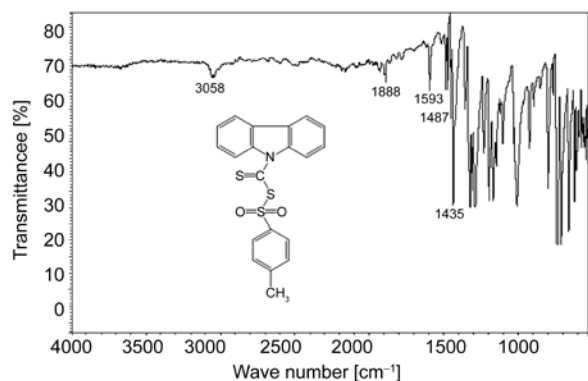


Figure 3. FTIR spectrum of 4-toluene 9*H*-carbazole-9-carbodithioate

aromatic CH), 8.09 (s, 1H, NH). ¹H-NMR peak difference between Cz and TCzC can be easily obtained as shown in Figure 4.

¹³C NMR (deuteriochloroform): δ 194.85; 139.85; 127.11; 126.14; 124.27; 120.37; 115.38; 77.34; 77.22; 77.02; 76.70. Analytically calculated for C₂₀H₁₅NO₂S₃ (397.53 g/mol) : C (71.01); H (4.72);

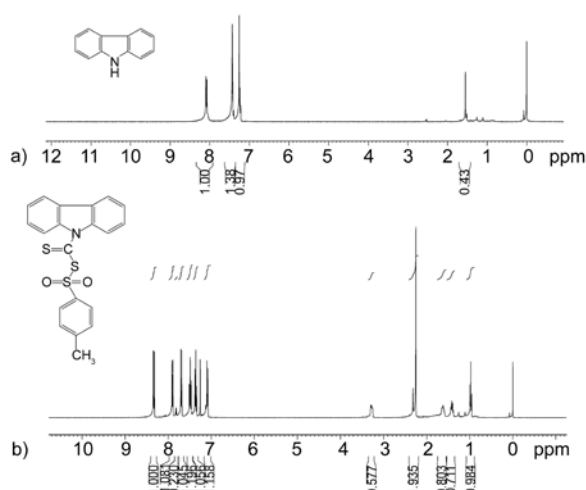


Figure 4. ¹H-NMR spectra of a) Cz and b) TCzC

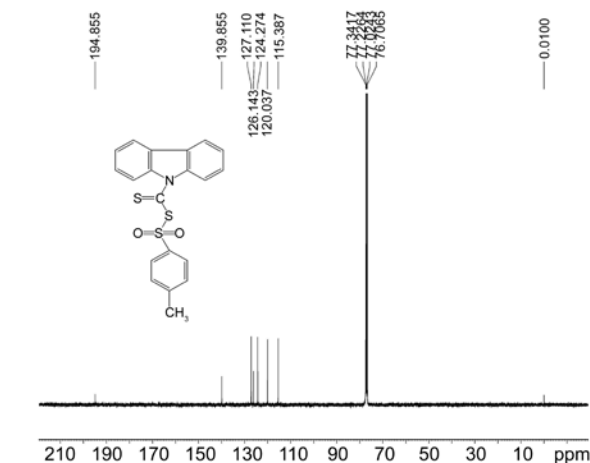
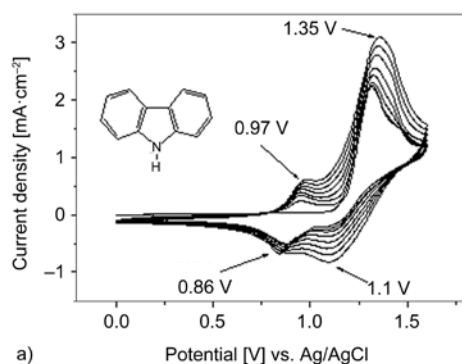


Figure 5. ¹³C-NMR spectrum of TCzC

N (4.72); O (4.36). Found: C (71.04); H (4.76); N (4.32) (Figure 5).

3.3. Electropolymerization of poly(4-toluene 9*H*-carbazole-9-carbodithioate)

In our previous study [41], electrogrowth of 9-tosyl-9*H*-carbazole on the carbon fiber microelectrode (CFME) was studied by CV at a scan rate of 100 mV·s⁻¹ at different initial monomer concentrations (1.0, 3.0, 5.0 and 10.0 mM) in 0.1 M NaClO₄/ACN. The anodic peak potential appeared at 0.78 V in the initial monomer concentration of 3.0 mM, which was a reversible process. When CS₂ group included into 9-tosyl-9*H*-carbazole structure, anodic peak potential was increased from 0.78 to 1.30 V. The peak at 0.97 V can only be attributed to the redox properties of the polymer P(Cz), not to carbazole, the monomer as shown in Figure 6. The total charge of PCz was obtained as 6.128 mC for 8th cycle during electrogrowth process. When tosyl functional group was added to the Cz structure, it increased the

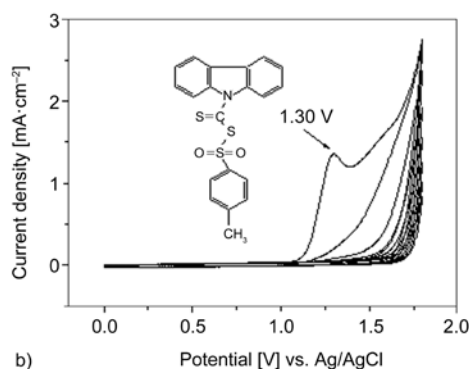


Figure 6. Cyclic voltammetry of a) Cz, [Cz]₀ = 3.0 mM (*Q* = 6.128 mC), b) TCzC, [TCzC]₀ = 3.0 mM (*Q* = 5.550 mC) on glassy carbon electrode (GCE) in 0.1 M TEABF₄/CH₂Cl₂-CH₃CN (8:2), 8 cycle, scan rate: 50 mV·s⁻¹, potential range: 0.0–1.8 V

$Q = 9.15$ mC. However, after addition of CS₂ group into the functional tosyl carbazole structure, the total charge decreased to $Q = 5.55$ mC during electro-growth process. The main reason of this decrease may be increasing of the length of the carbazole structure. Another important effect of the diffusion and migration of tetrafluoroborate and alkylammonium ions, which has important influence on the EIS. Therefore, P(TCzC) was difficult to electropolymerize compared to PCz on GCE.

3.4. Effect of scan rate in monomer-free solution

P(Cz) and P(TCzC) were immersed into a monomer-free electrolyte solution to check their redox behaviours. Scan rate was an important factor on the polymerization behavior. Modified polymer films were measured at the scan rate of 50, 100, 250, 500 and 1000 mV·s⁻¹ in monomer-free solution. The CVs peak potentials were similar for all scan rates with a small increase in current, which showed the doping and de-doping process of the polymer-coated GCE [41]. The peak current density (i_p) for a reversible voltammogram at 25°C is given by the following equation: $i_p = (2.69 \cdot 10^5) \cdot A \cdot D^{1/2} \cdot C_0 \cdot \nu^{1/2}$ where ν is the scan rate. A is the electrode area, D is the diffusion coefficient of electro-active species in the solution [42]. Peak current density is propor-

tional $\nu^{1/2}$ in the range of scan rates (Regression fit ($R_{An} = 0.99069$ and $R_{Cat} = -0.98381$) for P(Cz) and (Regression fit ($R_{An} = 0.9982$ and $R_{Cat} = -0.9972$) for P(TCzC)/GCE where diffusion control applies [43], respectively as given in Figures 7 and 8.

3.5. FTIR-ATR measurements

In FTIR-ATR spectrum of PCz and P(TCzC) were given in Figures 9 and 10. A significant band at 1090 cm⁻¹ has been attributed to BF₄⁻ ion for P(Cz), which is due to the electrolytes in TEABF₄. For the polymer, the band at 1600 cm⁻¹ could be assigned to the anti-symmetric and symmetric C–C stretching deformation. The peak at 3400 cm⁻¹ was obtained N–H stretching. The peak at 1230 and 720 cm⁻¹ corresponding to stretching of aromatic C–N bonds or vibration of disubstituted benzene ring and –C–H (out of plane deformation of C–H bond in benzene ring. P(TCzC) corresponds to peak at 3473 cm⁻¹ for C–H stretching, at 1626 cm⁻¹ for C=C stretching, at 1483 cm⁻¹ for CH₃, at 1046 cm⁻¹ for dopant ion (BF₄⁻) and at 762 cm⁻¹ for C–S stretching (Figure 10). The peak at 1156 cm⁻¹ was the bond of S=O bond in carbazole structure [44]. In our previous paper, PCz was electropolymerized on CFME in 0.1 M NaClO₄/PC. A significant band at 1093 cm⁻¹ was attributed to ClO₄⁻ ion. Other characteristic peaks at 3559, 1626, 1233 and 681–728 cm⁻¹ refer

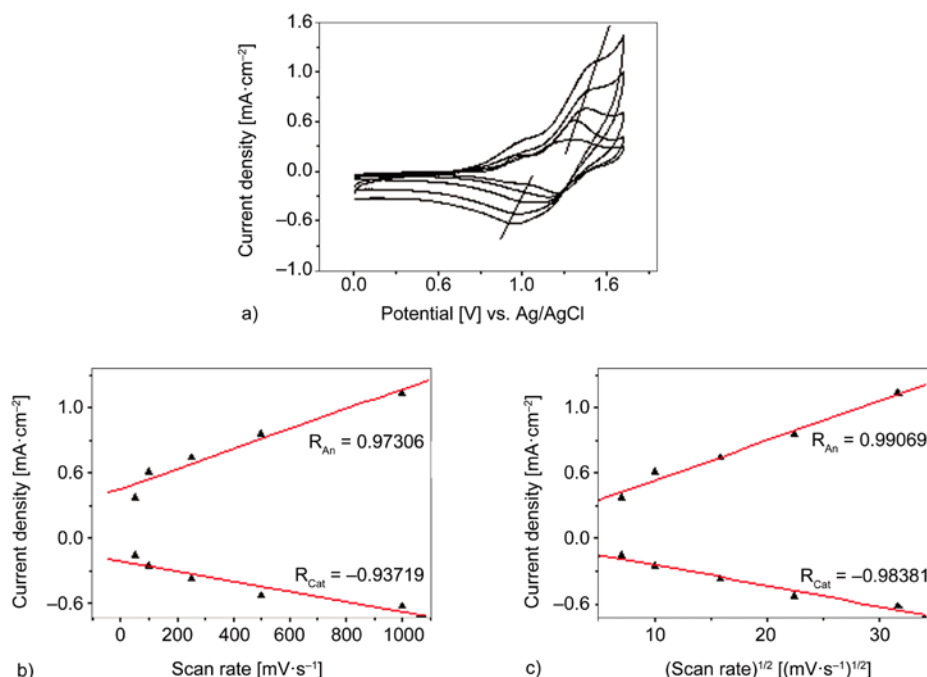


Figure 7. a) CV of PCz was obtained at different scan rates in monomer-free solution, b) scan rate vs. Current density, c) square root of scan rate vs. current density plots, CV was taken as 8 cycle, scan rate: 50–1000 mV·s⁻¹, potential range: 0–1.8 V in 0.1 M TEABF₄/CH₂Cl₂–CH₃CN (8:2), [Cz]₀ = 3.0 mM.

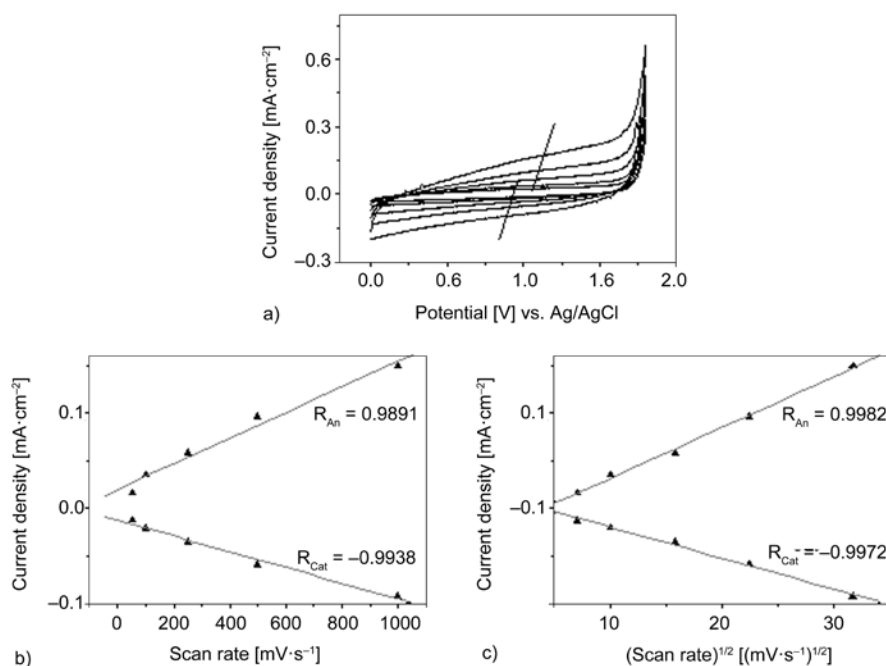


Figure 8. a) CV of P(TCzC) was obtained at different scan rates in monomer-free solution, b) scan rate vs. current density, c) square root of scan rate vs. current density plots, 8 cycle, scan rate: 50–1000 $\text{mV}\cdot\text{s}^{-1}$, potential range: 0–1.8 V in 0.1 M TEABF₄/CH₂Cl₂–CH₃CN (8:2), [TCzC]₀ = 3.0 mM

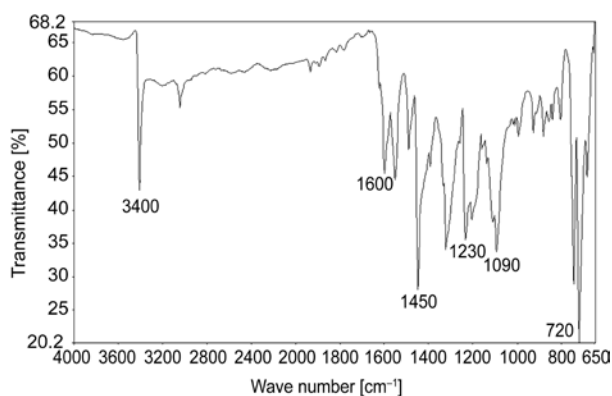


Figure 9. FTIR-ATR spectrum of P(Cz)/CFME in 0.1 M TEABF₄/CH₂Cl₂–CH₃CN (8:2)

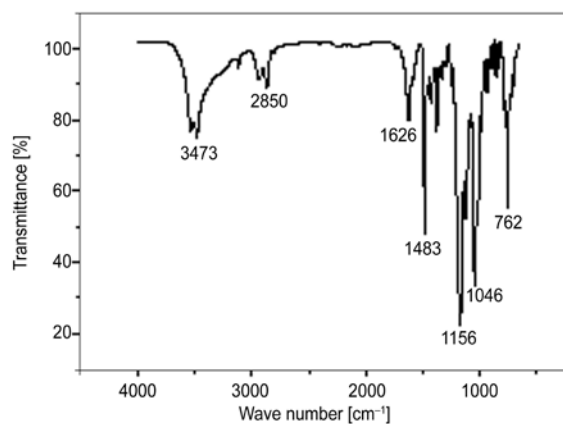


Figure 10. FTIR-ATR spectrum of P(TCzC)/CFME in 0.1 M TEABF₄/CH₂Cl₂–CH₃CN (8:2)

to $-\text{CH}_3$ (sp^3 CH str.), the anti-symmetric and symmetric C=C str. Deformation, $-\text{C}-\text{N}$ (str. of aromatic C–N bonds or vibrational of disubstituted benzene ring) and C–H (out of plane deformation of C–H bond in benzene ring) [45], respectively. PCz and P(TCzC) have different characteristic peaks to differentiate the functionality of polycarbazole.

3.6. SEM and AFM measurements

SEM micrograph of P(TCzC)/CFME was shown in Figure 11. Polymerization was performed on a single CFME (with diameter approximately 0.022 cm^2). Some pores of granules were shown on the CFME.

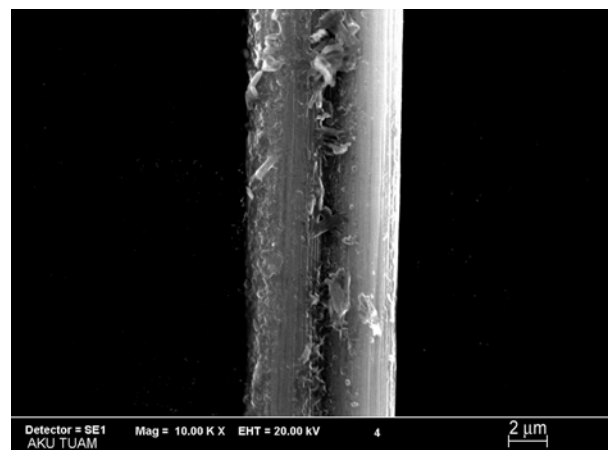


Figure 11. SEM images of P(TCzC)/CFME was performed in 0.1 M TEABF₄/CH₂Cl₂–CH₃CN (8:2) while the electropolymerization was carried out

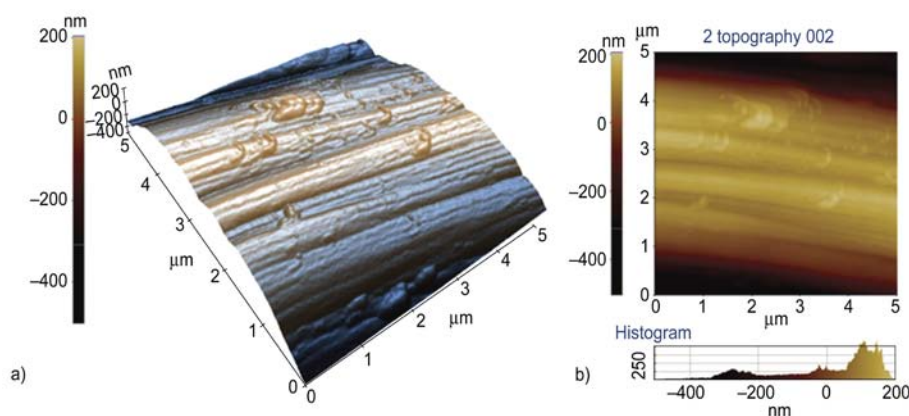


Figure 12. AFM analysis of P(TCzC)/CFME was performed in 0.1 M TEABF₄/CH₂Cl₂-CH₃CN(8:2) while the electro-polymerization was carried out

AFM images of P(TCzC)/CFME were obtained by fixing the fiber on a piece of silicon wafer with resin as shown in Figure 12. The AFM average roughness (R_q) value was obtained as 248.6 nm. AFM images of P(TCzC) was given in Figure 12. The electro-coating of modified electrodes was observed with granules on CFME. It was found in our previous study [46] from the cross-sectional analyses that striations of uncoated CFME with approximately 1 μm depth started disappearing and lower a thickness value of 50 nm. There is no doubt that average roughness value of uncoated CFME was increased ~ 5 times by electro-coating process. It is strong evidence of successful polymer formation provided by AFM analysis.

3.7. Electrochemical impedance spectroscopic study

Among electrochemical characterization techniques EIS represented useful results for the investigation of conducting polymers due to the small perturbations involved in the operative conditions for the impedance measurements [47, 48]. The impedance measurements, resistance was the real part and capacitance was calculated as $C = -1/(2\pi fZ''')$, where $\pi = 3.14$, f was frequency in Hz, and Z''' was the imaginary part of the impedance [49]. The low frequency capacitances (10 mHz) of P(Cz) ($C_{LF} = 1.44 \text{ mF}\cdot\text{cm}^{-2}$) and P(TCzC)/GCE ($C_{LF} = 0.43 \text{ mF}\cdot\text{cm}^{-2}$) were taken to identify the specific capacitance of polymer modified films. For lower frequencies, the spectra approached a nearly vertical line in the complex plane, which was typical of an ideal capacitor behavior. C_{LF} value decreased of 3.34 times by addition of CS₂ and tosyl group into the carbazole monomer (Figure 13a). In the Bode-phase plot, the maximum

phase angle was obtained as $\sim 65^\circ$ at the frequency of ~ 5 Hz as given in Figure 13b. The maximum capacitance value of P(TCzC)/GCE was obtained as $\sim 37 \mu\text{F}$ as shown in Figure 13c.

The model circuit comprised of eight elements, the solution resistance (R_s) was in series with the electrical double layer capacitance (C_{dl}) at the electrode and electrolyte. C_{dl} was in parallel with R_1 and (R_2 , W , and Q). The Warburg impedance was associated with the semi-infinite diffusion of ions in the electrode [50, 51]. The values of circuit parameters were estimated qualitatively from the fittings of experimental impedance spectra and presented for PCz/GCE in Table 1 and P(TCzC)/GCE in Table 2. The mean error of the modulus was $\sim 10\%$. The chi-squared (χ^2) was obtained as 10^{-3} and 10^{-4} for the circuit evaluations. χ^2 was the function defined as the sum of the squares of the residuals.

In literature, capacitors and supercapacitors are modeled by using many simple RC circuits. However, these models cannot accurately describe the voltage behavior of the modified polymer film and elec-

Table 1. Electrical equivalent circuit model of $R(C(R(Q(RW))))(CR)$, which is obtained for PCz/GCE

Circuit components	DC potential for PCz/GCE			
	-0.1 V	0.1 V	0.5 V	1.0 V
R_s [Ω]	360.7	313.0	300.3	313.2
C_{dl} [μF]	2.24	1.61	$4.54 \cdot 10^{-2}$	$6.21 \cdot 10^{-2}$
R_1 [Ω]	560.4	142.9	40.3	5.29
Q [$\mu\text{S}\cdot\text{s}^n$]	12.6	16.0	18.8	12.4
n	0.76	0.80	0.71	0.74
R_2 [Ω]	$1.29 \cdot 10^5$	$7.08 \cdot 10^4$	$3.18 \cdot 10^4$	202.3
W [$\mu\text{S}\cdot\text{s}^{-n}$]	18.0	36.8	144.0	21.7
C_{GCE} [μF]	0.624	0.041	43.5	0.94
R_{GCE} [Ω]	48.0	38.6	9924.0	1068.0
χ^2	$5.54 \cdot 10^{-4}$	$9.02 \cdot 10^{-4}$	$3.28 \cdot 10^{-4}$	$2.04 \cdot 10^{-3}$

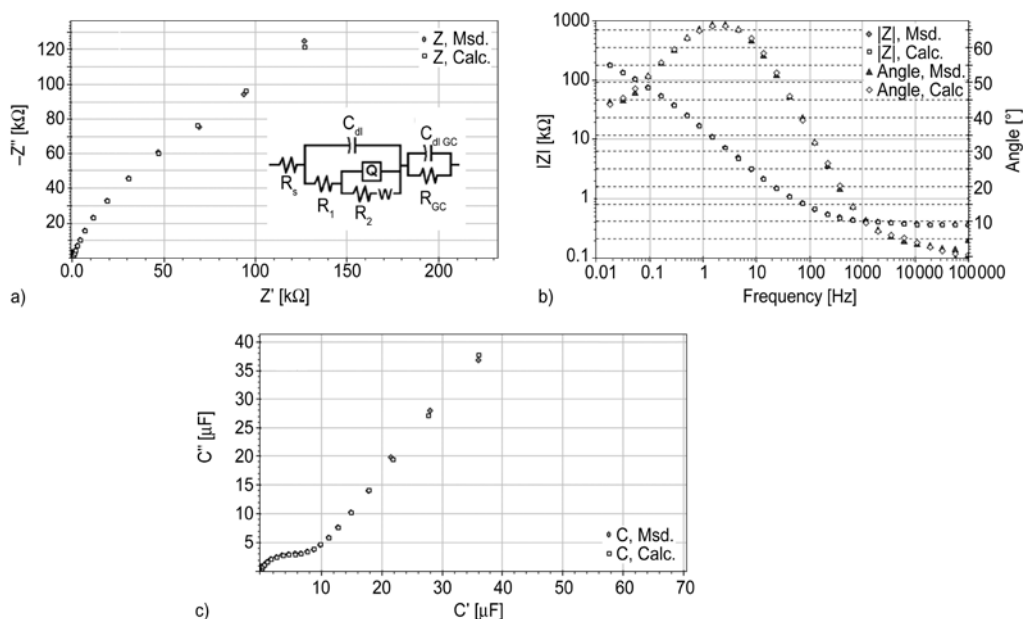


Figure 13. a) Nyquist graph inset: electrical equivalent circuit model of $R(C(R(Q(RW))))(CR)$, b) Bode magnitude and Bode-phase plot, c) capacitance graph of poly(TCzC) obtained by simulation ZSimpWin 3.10 program. Experiments were performed by simulation as the following conditions. $[TCzC]_0 = 3.0 \text{ mM}$, $0.1 \text{ M TEABF}_4/\text{CH}_2\text{Cl}_2\text{-CH}_3\text{CN}$ (8:2). Potential range was taken from 0 to 1.8 V.

Table 2. Electrical equivalent circuit model of $R(C(R(Q(RW))))(CR)$, which is obtained for P(TCzC)/GCE

Circuit components	DC Potential for P(TCzC)/GCE			
	-0.1 V	0.1 V	0.5 V	1.0 V
R_s [Ω]	381.8	216.0	342.2	330.8
C_{dl} [μF]	0.87	0.46	0.67	0.69
R_1 [Ω]	0.01	144.5	62.4	0.09
Q [$\mu\text{S}\cdot\text{s}^n$]	4.39	1.75	5.80	18.9
n	0.48	0.82	0.79	0.89
R_2 [Ω]	$3.82\cdot 10^6$	$7.53\cdot 10^4$	$1.47\cdot 10^5$	0.037
W [$\mu\text{S}\cdot\text{s}^{-n}$]	252.0	5.48	18.2	34.7
C_{GCE} [μF]	1.41	1.35	19.1	8.75
R_{GCE} [Ω]	67.4	147.0	3734.0	1026.0
χ^2	$1.06\cdot 10^{-3}$	$3.65\cdot 10^{-4}$	$3.14\cdot 10^{-4}$	$2.47\cdot 10^{-3}$

trolyte system [52, 53]. For fitting the data all capacitances in the equivalent circuit model of $R(C(R(Q(RW))))(CR)$ had to be replaced by a constant phase element CPE or Q [$Z_{CPE} = A_{CPE}(j\omega)^{-n}$] in order to adopt for non ideal behavior [54]. If $n = 1$ then $1/A_{CPE} = C$ with the dimension $\text{F}\cdot\text{cm}^{-2}$. The value of an ideal capacitance can be determined from the Bode plot of the impedance by extrapolating the measured capacitance with the slope $-n$ to the frequency $f = 1000 \text{ Hz}$ [55]. The highest n value of PCz was obtained as 0.80 at the DC potential of 0.1 V by applying EIS measurement. However, there were values as 0.82 and 0.89 for P(TCzC)/GCE system at the potential of 0.1 and 1.0 V, respectively. The highest double layer capacitance (C_{dl}) was obtained as

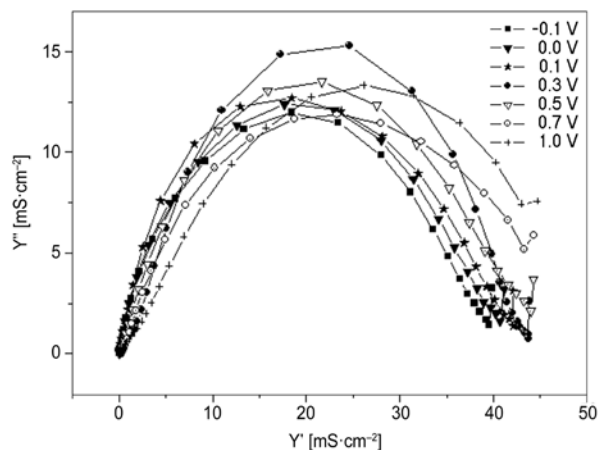


Figure 14. Admittance graph of P(TCzC) obtained by different DC potentials from -0.1 to 1.0 V. $[TCzC]_0 = 3.0 \text{ mM}$, $0.1 \text{ M TEABF}_4/\text{CH}_2\text{Cl}_2\text{-CH}_3\text{CN}$ (8:2). Potential range was taken from 0 to 1.8 V.

$2.24 \mu\text{F}$ for PCz and $0.87 \mu\text{F}$ for P(TCzC)/GCE at the DC potential of -0.1 V. R_1 and R_2 values decrease by increasing of DC potential of PCz. However, there was no systematic relation of P(TCzC)/GCE. The highest $R_1 = 144.5 \Omega$ at the DC potential of 0.1 V. However, $R_2 = 3.82 \text{ M}\Omega$ at the DC potential of -0.1 V.

The highest conductivity of P(TCzC)/GCE was obtained at the DC potential of 0.3 V for P(TCzC)/GCE as shown in Figure 14. There was an order from DC potential from -0.1 to 1.0 V. There was a deviation of 0.3 V for the P(TCzC)/GCE.

4. Conclusions

EIS was employed to characterize the capacitive behavior of electrochemically prepared novel synthesis of P(TCzC) film electrodes in organic electrolytes. The changing of polymer capacitance in dependence of the potential range from -0.1 to 1.0 V for PCz and P(TCzC)/GCE. C_{dl} was obtained as $2.24 \mu\text{F}$ for PCz and $0.87 \mu\text{F}$ for P(TCzC)/GCE at the DC potential of -0.1 V. And the resistance of GCE was obtained as $R_{GCE} = 9924 \Omega$ for PCz and $R_{GCE} = 3734 \Omega$ for P(TCzC) at the DC potential of 0.5 V. The double layer capacitance of P(TCzC) was lower than PCz. CS₂ group with tosyl group into Cz monomer decreased the capacitor behavior of the polymer.

Acknowledgements

This work was supported by The Scientific & Technological Council of Turkey (TUBITAK)-TBAG-110T791 Project. Authors also thank to Yakup Bakis (Fatih University, BINATAM, Istanbul, Turkey) for recording AFM images.

References

- [1] Gupta B., Singh A. K., Prakash R.: Electrolyte effects on various properties of polycarbazole. *Thin Solid Films*, **519**, 1016–1019 (2010). DOI: [10.1016/j.tsf.2010.08.034](https://doi.org/10.1016/j.tsf.2010.08.034)
- [2] Inzelt Gy.: Formation and redox behaviour of polycarbazole prepared by electropolymerization of solid carbazole crystals immobilized on an electrode surface. *Journal of Solid State Electrochemistry*, **7**, 503–510 (2003). DOI: [10.1007/s10008-003-0357-0](https://doi.org/10.1007/s10008-003-0357-0)
- [3] Du Y., Shen S. Z., Cai K. F., Casey P. S.: Research progress on polymer-inorganic thermoelectric nanocomposite materials. *Progress in Polymer Science*, **37**, 820–841 (2012). DOI: [10.1016/j.progpolymsci.2011.11.003](https://doi.org/10.1016/j.progpolymsci.2011.11.003)
- [4] Deng J., Guo L., Xiu Q., Zhang L., Wen G., Zhong C.: Two polymeric metal complexes based on polycarbazole containing complexes of 8-hydroxyquinoline with Zn(II) and Ni(II) in the backbone: Synthesis, characterization and photovoltaic applications. *Materials Chemistry and Physics*, **133**, 452–458 (2012). DOI: [10.1016/j.matchemphys.2012.01.064](https://doi.org/10.1016/j.matchemphys.2012.01.064)
- [5] Bussi re P-O., Rivaton A., Th rias S., Gardette J-L.: Multiscale investigation of the poly(*N*-vinylcarbazole) photoaging mechanism. *Journal of Physical Chemistry B*, **116**, 802–812 (2012). DOI: [10.1021/jp211358q](https://doi.org/10.1021/jp211358q)
- [6] Ates M., Uludag N., Karazehir T.: Copolymer formation of 9-(2-(benzyloxy)ethyl)-9*H*-carbazole and 1-tosyl-1*H*-pyrrole coated on glassy carbon electrode and electrochemical impedance spectroscopy. *Journal of Solid State Electrochemistry*, **16**, 2639–2649 (2012). DOI: [10.1007/s10008-012-1688-5](https://doi.org/10.1007/s10008-012-1688-5)
- [7] Stolar M., Baumgartner T.: Synthesis and unexpected halochromism of carbazole-functionalized dithienophospholes. *New Journal of Chemistry*, **36**, 1153–1160 (2012). DOI: [10.1039/c2nj40022g](https://doi.org/10.1039/c2nj40022g)
- [8] Gupta B., Joshi L., Prakash R.: Novel synthesis of polycarbazole–gold nanocomposite. *Macromolecular Chemistry and Physics*, **212**, 1692–1699 (2011). DOI: [10.1002/macp.201100262](https://doi.org/10.1002/macp.201100262)
- [9] Li S., Zhuang L-Q., George T. F.: Electric field-tuned polymer amplified spontaneous emission. *Journal of the Electrochemical Society*, **159**, P29–P34 (2012). DOI: [10.1149/2.001203jes](https://doi.org/10.1149/2.001203jes)
- [10] Pawar S. G., Chougule M. A., Sen S., Patil V. B.: Development of nanostructured polyaniline–titanium dioxide gas sensors for ammonia recognition. *Journal of Applied Polymer Science*, **125**, 1418–1424 (2012). DOI: [10.1002/app.35468](https://doi.org/10.1002/app.35468)
- [11] Booth M. A., Harbison S., Travas-Sejdic J.: Effects of redox couple on the response of polypyrrole-based electrochemical DNA Sensors. *Electroanalysis*, **24**, 1311–1317 (2012). DOI: [10.1002/elan.201200119](https://doi.org/10.1002/elan.201200119)
- [12] Drelinkiewicz A., Zi ba A., Solbezak J. W., Bonarawska M., Karpiński Z., Walksmundzka-G ra A., Stejskal J.: Polyaniline stabilized highly dispersed Pt nanoparticles: Preparation, characterization and catalytic properties. *Reactive and Functional Polymers*, **69**, 630–642 (2009). DOI: [10.1016/j.reactfunctpolym.2009.04.007](https://doi.org/10.1016/j.reactfunctpolym.2009.04.007)
- [13] Nie G., Xu J., Zhang S., Cai T., Han X.: Electrochemical copolymerization of carbazole and 3-methylthiophene. *Journal of Applied Polymer Science*, **102**, 1877–1885 (2006). DOI: [10.1002/app.24157](https://doi.org/10.1002/app.24157)
- [14] Huang M-R., Lu H-J., Li X-G.: Synthesis and strong heavy-metal ion sorption of copolymer microparticles from phenylenediamine and its sulfonate. *Journal of Materials Chemistry*, **22**, 17685–17699 (2012). DOI: [10.1039/c2jm32361c](https://doi.org/10.1039/c2jm32361c)
- [15] Li X-G., Feng H., Huang M-R., Gu G-L., Moloney M. G.: Ultrasensitive Pb(II) potentiometric sensor based on copolyaniline nanoparticles in a plasticizer-free membrane with a long lifetime. *Analytical Chemistry*, **84**, 134–140 (2012). DOI: [10.1021/ac2028886](https://doi.org/10.1021/ac2028886)
- [16] Li X-G., L  Q-F., Huang M-R.: Self-stabilized nanoparticles of intrinsically conducting copolymers from 5-sulfonic-2-anisidine. *Small*, **4**, 1201–1209 (2008). DOI: [10.1002/smll.200701002](https://doi.org/10.1002/smll.200701002)

- [17] Ates M., Uludag N., Karazehir T., Arican F.: A novel synthesis of 3,6-bis(2,3-dihydrothieno[3,4-b][1,4]dioxin-5-yl)-9-tosyl-9*H*-carbazole. *Ovidius University Annals of Chemistry*, **23**, 63–71 (2012).
DOI: [10.2478/v10310-012-0010-9](https://doi.org/10.2478/v10310-012-0010-9)
- [18] Uludag N., Ates M., Tercan B., Hökelek T.: 5-(3,6-dibromo-9*H*-carbazol-9-yl)pentanenitrile. *Acta Crystallographica Section E: Structure Report Online*, **67**, o642 (2011).
DOI: [10.1107/S1600536811005162](https://doi.org/10.1107/S1600536811005162)
- [19] Ates M., Uludag N., Sarac A. S.: Synthesis and electropolymerization of 9-tosyl-9*H*-carbazole, electrochemical impedance spectroscopic study and circuit modelling. *Fibers and Polymers*, **12**, 8–14 (2011).
DOI: [10.1007/s12221-011-0008-5](https://doi.org/10.1007/s12221-011-0008-5)
- [20] Ates M., Uludag N., Sarac A. S.: Electrochemical impedance of poly(9-tosyl-9*H*-carbazole-co-pyrrole) electrocoated carbon fiber. *Materials Chemistry and Physics*, **127**, 120–127 (2011).
DOI: [10.1016/j.matchemphys.2011.01.050](https://doi.org/10.1016/j.matchemphys.2011.01.050)
- [21] Lee H-Y, Chen G. S., Chen C-S., Chern J-W.: Efficient microwave-assisted synthesis of ellipticine through *N*-(1,4-dimethyl-9*H*-carbazol-3-ylmethyl)-*N*-tosylaminoacetaldehyde diethyl acetal. *Journal of Heterocyclic Chemistry*, **47**, 454–458 (2010).
DOI: [10.1002/jhet.319](https://doi.org/10.1002/jhet.319)
- [22] Hökelek T., Dal H., Tercan B., Gülle S., Ergün Y.: Ethyl 4-hydroxy-9-tosyl-9*H*-carbazole-3-carboxylate. *Acta Crystallographica Section E: Structure Reports Online*, **65**, o1515–o1516 (2009).
DOI: [10.1107/S1600536809021035](https://doi.org/10.1107/S1600536809021035)
- [23] Gu Y., Chen W-Q., Wada T., Hashizume D., Duan X-M.: From supermolecular sheet to helix by breaking molecular symmetry: the case of 4-[2-(carbazol-3-yl)vinyl] pyridium tosylate. *CrystEngComm*, **9**, 541–544 (2007).
DOI: [10.1039/b701377a](https://doi.org/10.1039/b701377a)
- [24] Martínez-Espérón M. F., Rodríguez D., Castedo L., Saá C.: Coupling and cycloaddition of ynamides: homo- and Negishi coupling of tosylynamides and intramolecular [4+2] cycloaddition of *N*-(*o*-ethynyl)phenyl ynamides and arylynamides. *Tetrahedron*, **62**, 3843–3855 (2006).
DOI: [10.1016/j.tet.2005.11.082](https://doi.org/10.1016/j.tet.2005.11.082)
- [25] Ates M., Uludag N.: Synthesis of 9-(4-nitrophenylsulfonyl)-9*H*-carbazole: Comparison of an impedance study of poly[9-(4-nitrophenylsulfonyl)-9*H*-carbazole] on gold and carbon fiber microelectrodes. *Journal of Applied Polymer Science*, **124**, 4655–4662 (2012).
DOI: [10.1002/app.35380](https://doi.org/10.1002/app.35380)
- [26] Beaujuge P. M., Reynolds J. R.: Color control in π -conjugated organic polymers for use in electrochromic devices. *Chemical Reviews*, **110**, 268–320 (2010).
DOI: [10.1021/cr900129a](https://doi.org/10.1021/cr900129a)
- [27] Kötz R., Hahn M., Gally R.: Temperature behavior and impedance fundamentals of supercapacitors. *Journal of Power Sources*, **154**, 550–555 (2006).
DOI: [10.1016/j.jpowsour.2005.10.048](https://doi.org/10.1016/j.jpowsour.2005.10.048)
- [28] Vorotyntsev M. A., Daikhin L. I., Levi M. D.: Modeling the impedance properties of electrodes coated with electroactive polymer films. *Journal of Electroanalytical Chemistry*, **364**, 37–49 (1994).
DOI: [10.1016/0022-0728\(93\)02957-J](https://doi.org/10.1016/0022-0728(93)02957-J)
- [29] Inzelt G., Pineri M., Schultze J. W., Vorotyntsev M. A.: Electron and proton conducting polymers: recent developments and prospects. *Electrochimica Acta*, **45**, 2403–2421 (2000).
DOI: [10.1016/S0013-4686\(00\)00329-7](https://doi.org/10.1016/S0013-4686(00)00329-7)
- [30] Aravinda L. S., Bhat K. U., Bhat B. R.: Nano CeO₂/activated carbon based composite electrodes for high performance supercapacitor. *Materials Letters*, **112**, 158–161 (2013).
DOI: [10.1016/j.matlet.2013.09.009](https://doi.org/10.1016/j.matlet.2013.09.009)
- [31] Yang J. E., Jang I., Kim M., Baeck S. H., Hwang S., Shim S. E.: Electrochemically polymerized vine-like nanostructured polyaniline on activated carbon nanofibers for supercapacitor. *Electrochimica Acta*, **111**, 136–143 (2013).
DOI: [10.1016/j.electacta.2013.07.183](https://doi.org/10.1016/j.electacta.2013.07.183)
- [32] Zhang L. L., Zhao X. S.: Carbon-based materials as supercapacitor electrodes. *Chemical Society Reviews*, **38**, 2520–2531 (2009).
DOI: [10.1039/b813846j](https://doi.org/10.1039/b813846j)
- [33] Li C., Wang D., Liang T., Wang X., Ji L.: A study of activated carbon nanotubes as double-layer capacitors electrode materials. *Materials Letters*, **58**, 3774–3777 (2004).
DOI: [10.1016/j.matlet.2004.07.027](https://doi.org/10.1016/j.matlet.2004.07.027)
- [34] Hwang S-G., Ryu S-H., Yun S-R., Ko J. M., Kim K. M., Ryu K-S.: Behavior of NiO–MnO₂/MWCNT composites for use in a supercapacitor. *Materials Chemistry and Physics*, **130**, 507–512 (2011).
DOI: [10.1016/j.matchemphys.2011.07.022](https://doi.org/10.1016/j.matchemphys.2011.07.022)
- [35] Kuang H., Cao Q., Wang X., Jing B., Wang Q., Zhou L.: Influence of the reaction temperature on polyaniline morphology and evaluation of their performance as supercapacitor electrode. *Journal of Applied Polymer Science*, **130**, 3753–3758 (2013).
DOI: [10.1002/app.39650](https://doi.org/10.1002/app.39650)
- [36] He X., Gao B., Wang G., Wei J., Zhao C.: A new nanocomposite: Carbon cloth based polyaniline for an electrochemical supercapacitor. *Electrochimica Acta*, **111**, 210–215 (2013).
DOI: [10.1016/j.electacta.2013.07.226](https://doi.org/10.1016/j.electacta.2013.07.226)
- [37] Lu T., Zhang Y., Li H., Pan L., Li Y., Sun Z.: Electrochemical behaviors of graphene–ZnO and graphene–SnO₂ composite films for supercapacitors. *Electrochimica Acta*, **55**, 4170–4173 (2010).
DOI: [10.1016/j.electacta.2010.02.095](https://doi.org/10.1016/j.electacta.2010.02.095)
- [38] Zhi M., Xiang C., Li J., Li M., Wu N.: Nanostructured carbon–metal oxide composite electrodes for supercapacitors: A review. *Nanoscale*, **5**, 72–88 (2013).
DOI: [10.1039/c2nr32040a](https://doi.org/10.1039/c2nr32040a)

- [39] Zhou D., Zhu X. L., Zhu J., Yin H. S.: Influence of the chemical structure of dithiocarbamates with different *N*-groups on the reversible addition–fragmentation chain transfer polymerization of styrene. *Journal of Polymer Science Part A: Polymer Chemistry*, **43**, 4849–4856 (2005).
DOI: [10.1002/pola.20947](https://doi.org/10.1002/pola.20947)
- [40] Xue X., Zhu J., Zhang Z., Cheng Z., Tu Y., Zhu X.: Synthesis and characterization of azobenzene-functionalized poly(styrene)-*b*-poly(vinyl acetate) via the combination of RAFT and ‘click’ chemistry. *Polymer*, **51**, 3083–3090 (2010).
DOI: [10.1016/j.polymer.2010.04.052](https://doi.org/10.1016/j.polymer.2010.04.052)
- [41] Sarac A. S., Evans U., Serantoni M., Cunnane V. J.: Electrochemical and morphological study of the effect of polymerization conditions on poly(tetrathiothiophene) with emphasis on carbon fiber microelectrodes: A cyclic voltammetry and atomic force microscopy study. *Carbon*, **41**, 2725–2730 (2003).
DOI: [10.1016/S0008-6223\(03\)00331-2](https://doi.org/10.1016/S0008-6223(03)00331-2)
- [42] Sarac A. S., Ates M., Parlak E. A.: Electrolyte and solvent effects of electrocoated polycarbazole thin films on carbon fiber microelectrodes. *Journal of Applied Electrochemistry*, **36**, 889–898 (2006).
DOI: [10.1007/s10800-006-9145-8](https://doi.org/10.1007/s10800-006-9145-8)
- [43] Rusling J. F., Suib S. L.: Characterizing materials with cyclic voltammetry. *Advanced Materials*, **6**, 922–930 (1994).
DOI: [10.1002/adma.19940061204](https://doi.org/10.1002/adma.19940061204)
- [44] Sarac A. S., Sezgin S., Ates M., Turhan C. M.: Electrochemical impedance spectroscopy and morphological analyses of pyrrole, phenylpyrrole and methoxyphenylpyrrole on carbon fiber microelectrodes. *Surface and Coatings Technology*, **202**, 3997–4005 (2008).
DOI: [10.1016/j.surfcoat.2008.02.007](https://doi.org/10.1016/j.surfcoat.2008.02.007)
- [45] Papež V., Inganäs O., Cimrová V., Nešpůrek S.: Electrochemical preparation and study of thin poly(*N*-vinylcarbazole) layers. *Journal of Electroanalytical Chemistry and Interfacial Electrochemistry*, **282**, 123–139 (1990).
DOI: [10.1016/0022-0728\(91\)85093-5](https://doi.org/10.1016/0022-0728(91)85093-5)
- [46] Sarac A. S., Sezgin S., Ates M., Turhan M. C.: Monomer concentration effect on electrochemically modified carbon fiber with poly[1-(4-methoxyphenyl)-1*H*-pyrrole] as microcapacitor electrode. *Advances in Polymer Technology*, **28**, 120–130 (2009).
DOI: [10.1002/adv.20152](https://doi.org/10.1002/adv.20152)
- [47] Musiani M. M.: Characterization of electroactive polymer layers by electrochemical impedance spectroscopy (EIS). *Electrochimica Acta*, **35**, 1665–1670 (1990).
DOI: [10.1016/0013-4686\(90\)80023-H](https://doi.org/10.1016/0013-4686(90)80023-H)
- [48] Tarola A., Dini D., Salatelli E., Andreani F., Decker F.: Electrochemical impedance spectroscopy of polyalkylterthiophenes. *Electrochimica Acta*, **44**, 4189–4193 (1999).
DOI: [10.1016/S0013-4686\(99\)00133-4](https://doi.org/10.1016/S0013-4686(99)00133-4)
- [49] Miller J. R., Outlaw R. A., Holloway B. C.: Graphene electric double layer capacitor with ultra-high-power performance. *Electrochimica Acta*, **56**, 10443–10449 (2011).
DOI: [10.1016/j.electacta.2011.05.122](https://doi.org/10.1016/j.electacta.2011.05.122)
- [50] Sen P., De A.: Electrochemical performances of poly(3,4-ethylenedioxythiophene)–NiFe₂O₄ nanocomposite as electrode for supercapacitor. *Electrochimica Acta*, **55**, 4677–4684 (2010).
DOI: [10.1016/j.electacta.2010.03.077](https://doi.org/10.1016/j.electacta.2010.03.077)
- [51] Conway B. E.: *Electrochemical supercapacitors, scientific fundamentals and technological applications*. Kluwer Academic/Plenum Publishers, New York (1999).
- [52] Mahon P. J., Paul G. L., Keshishian S. M., Vassallo A. M.: Measurement and modelling of the high-power performance of carbon-based supercapacitors. *Journal of Power Sources*, **91**, 68–76 (2000).
DOI: [10.1016/S0378-7753\(00\)00488-2](https://doi.org/10.1016/S0378-7753(00)00488-2)
- [53] Buller S., Karden E., Kok D., De Donker R. W.: Modeling the dynamic behavior of supercapacitors using impedance spectroscopy. *IEEE Transactions on Industry Applications*, **38**, 1622–1626 (2002).
DOI: [10.1109/TIA.2002.804762](https://doi.org/10.1109/TIA.2002.804762)
- [54] Rammelt U., Reinhard G.: On the applicability of a constant phase element (CPE) to the estimation of roughness of solid metal electrodes. *Electrochimica Acta*, **35**, 1045–1049 (1990).
DOI: [10.1016/0013-4686\(90\)90040-7](https://doi.org/10.1016/0013-4686(90)90040-7)
- [55] Fikus A., Rammelt U., Plieth W.: Characterization of semiconductor properties of polybithiophene film electrodes in contact with aqueous electrolytes. A combination of electrochemical impedance spectroscopy and photocurrent measurements. *Electrochimica Acta*, **44**, 2025–2035 (1999).
DOI: [10.1016/S0013-4686\(98\)00311-9](https://doi.org/10.1016/S0013-4686(98)00311-9)